ISSN 2669-2023 (print) / ISSN 2538-8959 (on-line) / **https://doi.org/10.47459/cndcgs.2026.143**

Simulation Analysis of the Combined Effects of Counter-mobility Measures and Firepower in Military Operations

Tibor PALASIEWICZ[1]*, Michal BILINA[1], Pavel ŽIŽKA[1], Jaroslav ZÁLESKÝ[1]

[1]Department of Engineer Support, Faculty of Military Leadership, University of Defence, Address: Kounicova 65, 662 10, Brno, Czech Republic

*Correspondence:*tibor.palasiewicz@unob.cz*

Abstract

Obstacles alone may not be sufficient to stop or destroy a target completely, but they can degrade its mobility. This helps to make firepower more effective. This study examines when using both counter-mobility measures (CM) and firepower effects (JF) together yields greater effectiveness than using them separately. Monte Carlo simulations in MATLAB 2025a were used to compare CM, JF, and CM+JF. The comparison is based on the probability of detection (*PD*) and the weapon system availability rate (*WSAR*). Synergy is measured in two ways: (i) D_{diff}, which shows how many more targets are destroyed with CM+JF compared to using CM and JF separately, and (ii) the index *S*, which shows the total effect of CM+JF compared to the sum of the CM and JF effects. The results showed positive synergy in most cases, with 44 of the 50 combinations having a positive lower bound for the 95% confidence intervals of D_{diff}.

KEY WORDS: *counter-mobility measures, enemy delay, firepower, integrated defense, Monte Carlo method, multi-domain operations, non-additivity, simulation experiment, synergy*

Citation: Palasiewicz, T.; Bilina, M.; Žižka, P.; Záleský J. Simulation analysis of the combined effects of counter-mobility measures and firepower in military operations. In Proceedings of the Challenges to National Defence in Contemporary Geopolitical Situation, Brno, Czech Republic, 07 – 10 September 2026. ISSN 2538-8959, https://doi.org/10.47459/cndcgs.2026.143

1. Introduction

The current conflicts and security environment underscore the necessity of a defense system capable of producing decisive outcomes under conditions characterized by high dynamics, significant disruption, and rapid adversary adaptation [1]. Within the framework of an alliance strategy, the focus is on harmonizing activities across operational domains to achieve convergent effects, enabling the defense system to concentrate these effects at the optimal time and location, thereby exploiting the adversary's fleeting vulnerabilities [2].

In land operations, counter-mobility measures and firepower are two fundamental components of defense. Counter-mobility measures modify the battlefield's geometry and influence the tempo of the adversary maneuvers by restricting their freedom of movement, directing maneuvers into predetermined paths, and creating a temporal opportunity for effective engagement [3]. Doctrinally, the objectives of obstacles are articulated through a series of intended effects, including disrupting, turning, fixing, and blocking the enemy's advance [4; 5].

Fires, conversely, serve as a mechanism to induce the desired alterations in the adversary's behavior and capabilities [6], encompassing a spectrum ranging from physical destruction to non-lethal effects. The fire support doctrine explicitly states that fires are systematically planned and executed to achieve synergistic outcomes, with the integration of target acquisition, command and control, and fire assets playing a pivotal role [7].

Although doctrinal principles emphasize integration, the practical evaluation of the effects of combined actions is frequently reduced to the additive aggregation of the individual components. However, this approach may inadequately represent the nonlinear relationships among target retention time, decision-making cycle speed, and strike effectiveness. In numerous instances, defense demonstrates the characteristics of a complex adaptive system, where the resultant effect is not merely the sum of individual performances but emerges from their interactions, feedback loops, and temporal sequencing [8].

The objective of this study is to quantify the non-additive component of the effect of combined defense strategies, specifically counter-mobility (CM) measures and joint fires (JF), and to identify the conditions under which this non-additivity becomes practically significant. The methodology involves a simulation experiment in which two critical parameters are systematically varied: (i) target detection and tracking quality, represented by the *PD* parameter, and (ii) fire availability and activation, represented by the *WSAR* parameter. Non-additivity is assessed using the D_{diff} metric and synergy index *S*, as formally defined in the Methodology section. The findings are presented as sensitivity maps and are supported by a statistical evaluation of robustness.

2. Literature Review

Doctrinal literature concurs that obstacles serve not as an end in themselves, but as a means to influence the adversary maneuver and establish favorable conditions for subsequent actions against them. Within the context of joint operations, the obstacle system is perceived as a tool intended to achieve specific effects, such as disruption, fixation, turning, or blocking, thereby creating a scenario in which other assets can attain enhanced operational effectiveness [4; 5].

Fire effects are doctrinally characterized as the employment of weapon systems to achieve intended effects, both lethal and non-lethal, on a target. These effects are integrated into a comprehensive system that encompasses target acquisition, command and control, and fire support assets. The doctrine further underscores that the planning and execution of fires focus on synchronization and integration with other activities to attain synergistic outcomes [7].

Within the context of NATO, this principle is integrated into the comprehensive framework of land operations conducted in a multinational and joint setting, highlighting the importance of coordinating and mutually enhancing capabilities during the planning and execution of land operations [9]. From a procedural perspective, a critical interface between detection and engagement is the targeting system, which, according to the alliance doctrine, delineates the roles, responsibilities, and steps required to engage targets to achieve effects [10; 11; 12].

The prevailing methodology for assessing the impact of obstacles and firepower typically treats these elements as distinct entities; however, it also underscores the necessity for their integration, given their mutual influence in practical scenarios [4; 13; 14]. Obstacles can affect not only the rate of advancement but also the density, configuration, and predictability of targets, thereby impacting the efficacy of the firepower [15; 16]. Consequently, the critical determinant is not merely the magnitude of the delay induced but whether this delay can be effectively leveraged within the command-and-control decision-making cycle and whether there exists a sufficiently swift connection between detection and engagement. This focus on prompt responsiveness aligns with contemporary initiatives to reduce the sensor-to-shooter interval as part of the modernization of command and control, which encompasses data integration, automation, and decision support [17].

In this context, it is beneficial to introduce metrics that explicitly quantify the enhancement effect resulting from integration, as opposed to a hypothetical additive composition. These metrics facilitate not only the identification of non-additivity but, more importantly, enable the comparison of different defense system variants based on the conditions under which the non-additive contribution is of practical significance.

The behavior of combat systems is frequently characterized by nonlinearity, sensitivity to initial conditions, and the influence of actors' adaptations [18]. Consequently, purely deterministic calculations may be inadequate for evaluating integrated systems. The theory of complex adaptive systems is employed in defense analyses as a framework to describe scenarios in which outcomes emerge from the interactions of numerous elements and where emergent phenomena are observed [8].

Simulation methodologies, particularly agent-based modeling, are employed in this context to encapsulate local interactions, adaptation, and behavioral variability, as well as to estimate the distribution of outcomes rather than their mean values. Within the defense sector, there are instances of utilizing agent-based approaches to model combat scenarios as complex adaptive systems and to investigate the impact of "soft" factors or informational links (e.g., methodological contributions from the field of simulation science and defense modeling) [19; 20; 21].

This study advances this area of research by employing a simulation experiment to quantify the non-additive component of the integrated effects. Its distinct contribution is the systematic exploration of the parameter space of *PD* and *WSAR*, along with the introduction of the metrics D_{diff} and *S*. These metrics facilitate the interpretation of non-additivity as both a relative phenomenon (the synergy index *S*) and an absolute increase in effect (D_{diff}). This approach effectively bridges the doctrinal assertion of synergy with a quantitative and statistically grounded evaluation.

3. Methodology

The problem under consideration involves nonlinear relationships among the delaying effect of obstacles, adversary adaptation, and time-dependent fires. For this reason, the Monte Carlo simulation method was selected, as it allows stochastic events to be incorporated and the resulting differences between operational modes to be quantified (counter-mobility measures only, fires only, and their combination) [13; 14; 22]. The calculations were performed in MATLAB 2025a.

3.1 Modelled Scenario and Definition of the CM and JF Components

The simulation captures the penetration of an armored vehicle column through an area containing an obstacle (CM) and subject to simultaneous fires (JF). A minefield is used as a representative obstacle element, the effect of which is manifested in two ways: (i) direct vehicle losses incurred when attempting to pass through without first creating a breach, and (ii) a time delay arising when the unit shifts to obstacle breaching.

For the purposes of the model, the column is assumed to advance toward the obstacle area at a speed of 30 km/h. If the third vehicle is destroyed as a result of the obstacle effect, a transition to the obstacle-breaching mode is triggered: the remaining vehicles halt, withdraw at low speed (on the order of a few kilometers per hour), after which breach creation takes place (modelled as a random delay in the range of 10–20 minutes), followed by alignment into the breach (fixed delay of 5 minutes), passage through the breach at reduced speed (approximately 15 km/h), and, after crossing the obstacle, redeployment (fixed delay of 3 minutes). This temporal structure creates, for some targets, a period of limited mobility or complete halt, which is decisive for the effectiveness of fires.

In the model, JF fires are represented by the probabilistic neutralization of targets, with effectiveness differentiated between moving targets and stationary (or significantly slowed) targets. The baseline effectiveness of a single fire is set at 0.30 for a moving target and 0.50 for a stationary target. The overall effectiveness of JF is further governed by the *PD* and *WSAR* parameters (see below), which jointly determine the probability that a target is detected, localized, and engaged effectively in time. The number of fire assets is not introduced explicitly in the model. Instead, their availability and ability to engage in a timely manner are represented by the aggregated *WSAR* parameter, which thus encompasses both the available fire capacity and the ability to allocate targets and deliver an engagement within the required time frame.

The key scenario and simulation settings are summarized in Table 1. The table presents the number of targets in the column, the speed and time components associated with obstacle breaching, the rule governing the transition to breach creation after the third loss, and the probabilities of target neutralization by fires for moving and stationary targets. It also includes the control parameters *PD* and *WSAR*, as well as the simulation parameters (*R*, *B*).

Table 1.

Scenario and Simulation Parameters

Group	**Parameter**	**Symbol / Value**	**Note**
Convoy	Number of vehicles/targets in the column	$N = 50$	Number of targets modelled in a single penetration episode
	Speed of advance before the obstacle	30 km/h	Standard speed of forward movement
Obstacle (CM)	Probability of destruction during an attempt to pass through without prior breaching	0.50	Applies only until the transition to obstacle breaching
Tactical Rule	Trigger for transition to obstacle breaching	3rd vehicle destroyed	Once the third vehicle is destroyed, the convoy halts and transitions to breaching mode
Withdrawal	Reverse withdrawal speed	5 km/h	Indicative value for reversing
Breaching	Time required to create a breach	10–20 min	Randomly selected within the specified interval
	Time required to align into the breach	5 min	Fixed time component
	Speed of passage through the breach	15 km/h	Reduced speed during passage
Post-Breaching	Redeployment time after passing through the breach	3 min	Fixed time component
Fires (JF)	Effectiveness against a moving target	0.30	Probability of neutralizing a moving target by a single fire
	Effectiveness against a stationary target	0.50	Probability of neutralizing a stationary target by a single fire
	Fire assets	Represented by the aggregated *WSAR* parameter	The number of assets is not modelled explicitly; *WSAR* represents both the available fire capacity and the ability to deliver timely engagement
Control Parameter	Target detection and tracking quality	*PD*	Varied across the parameter grid (see 3.2)
	Fire availability and activation	*WSAR*	Varied across the parameter grid (see 3.2)
Simulation	Number of replications at each grid point	$R = 1500$	Paired replications for the CM, JF, and CM+JF modes
Statistics	Number of bootstrap resamples	$B = 7000$	Paired bootstrap with percentile 95% confidence intervals
Implementation	Simulation environment	MATLAB 2025a	Monte Carlo simulation

3.2 Control Parameters and Experimental Grid

The numerical experiments were conducted over a grid of two controlled parameters:

1. *PD* – the probability of detecting the target and maintaining target information (including its transfer into the fire chain), understood in the simulation as an aggregated parameter of detection quality and target data transmission;
2. *WSAR* – a normalised coefficient of fire availability and effective fires, aggregating the availability of fire assets, the ability to allocate targets, and the capability to deliver effective fire under the given conditions.

The parameters are varied over a discrete grid: $PD \in \{0.0; 0.1; \ldots; 0.9\}$ and $WSAR \in \{0.10; 0.25; 0.50; 0.75; 1.00\}$. At each grid point, three operational modes are simulated: CM only, JF only, and the combined CM+JF mode.

3.3 Simulation Procedure and Implementation

The computations were performed using the Monte Carlo method in MATLAB 2025a. Each grid point (*PD*, *WSAR*) was evaluated by means of $R = 1500$ independent replications. Within a single replication, results were generated for the three modes (CM, JF, and CM+JF) under identical initial scenario conditions (the same number of targets and the same scheme of advance). This ensures that differences between the modes arise primarily from the effects of the modelled mechanisms rather than from changes in the input conditions.

The output of a single replication consists of three values: the number of targets destroyed in the CM mode, the JF mode, and the CM+JF mode. For selected grid points, the outputs are stored in tabular form, with three columns corresponding to these modes.

3.4 Evaluated Metrics

The primary performance measure is the number of targets destroyed per replication. For each grid point, the following mean values are derived from the replications:

1. D_{CM} – the mean number of targets destroyed under CM-only conditions;
2. D_{JF} – the mean number of targets destroyed under JF-only conditions;
3. D_{CM+JF} – the mean number of targets destroyed under the simultaneous application of CM and JF.

The synergistic effect is quantified by two complementary metrics:

1. Absolute synergy

$$D_{\mathrm{diff}} = D_{\mathrm{CM+JF}} - \left(D_{\mathrm{CM}} + D_{\mathrm{JF}}\right), \qquad (1)$$

where a positive value of D_{diff} indicates a non-additive effect; that is, the combination of the obstacle and fires produces a stronger effect than would correspond to the simple sum of their individual effects.

2. Synergy index

The synergy index *S* is defined at the level of an individual replication as the ratio of the combined effect to the sum of the individual effects:

$$S = \frac{D_{\mathrm{CM+JF}}}{D_{\mathrm{CM}} + D_{\mathrm{JF}} + \varepsilon}, \qquad (2)$$

where ε is a very small positive number introduced solely for numerical reasons (to prevent division by zero in edge cases). For each grid point, the mean value of *S* across all replications is then reported.

3.5 Statistical Processing, Confidence Intervals, and p-Values

The robustness of the estimates is assessed using bootstrap resampling with replacement at the level of replications. For each grid point, $B = 7000$ resamples are generated, and 95% confidence intervals are derived from the empirical distribution of the estimates using the percentile method.

The values of D_{CM}, D_{JF}, and D_{CM+JF} are generated within the same replication under identical initial scenario conditions; therefore, the resampling procedure is performed in a paired manner. In each bootstrap step, entire triplets (CM, JF, CM+JF) are sampled according to the replication indices. The metrics D_{diff} and *S* are then recalculated from the resampled data, and their confidence intervals are subsequently derived.

The significance test for synergy is formulated for the null hypothesis H0 : $D_{\mathrm{diff}} \leq 0$ against the alternative hypothesis H1 : $D_{\mathrm{diff}} > 0$. The one-sided p-value is estimated as the proportion of bootstrap realizations for which $D_{\mathrm{diff}}* \leq 0$. For completeness, a two-sided p-value may also be reported as $2\min(p, 1 - p)$, where p denotes the one-sided value.

4. Results

The results were evaluated over the *PD* × *WSAR* parameter grid. The basic comparison of the three modes (CM, JF, and CM+JF) shows that the CM+JF combination leads, across most of the parameter space, to a substantially higher number of targets destroyed than the individual application of either component alone. The mean number of targets destroyed ranged from 0.96 to 3.23 per simulation run in the CM mode, from 1.10 to 6.03 in the JF mode, and from 2.37 to 27.36 in the CM+JF mode.

Absolute synergy, expressed by the metric (1), increased with increasing values of *PD* and *WSAR* (Fig. 1). Across most of the parameter grid, the synergy was not only positive on average but also statistically supported: the lower bound of the 95% confidence interval for D_{diff} was greater than zero in 44 out of 50 parameter combinations. The confidence intervals were estimated using a paired bootstrap (percentile method). The exceptions were concentrated in the region of very low *PD* values, where D_{diff} remained close to zero and the confidence intervals also included negative values (i.e., under these conditions, positive absolute synergy was not demonstrated).

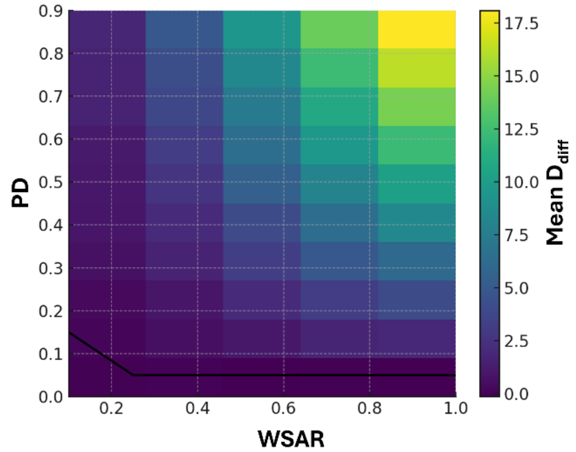

Fig. 1. Mean absolute synergy D_{diff} over the *PD* × *WSAR* parameter grid.

The color scale shows the mean value of absolute synergy across the grid of combinations of *PD* and *WSAR*. Higher values of D_{diff} indicate a stronger non-additive effect of the combination of obstacles and fires, i.e., situations in which the combined action exceeds the simple sum of the partial effects. The values are aggregated across model replications. The map shows that D_{diff} increases with increasing *WSAR* and, simultaneously, with increasing *PD*.

The multiplicative perspective, expressed through the synergy index *S*, yielded values greater than 1 across the entire parameter grid. The mean values of *S* ranged approximately from 1.17 to 3.33, while the lower bounds of the 95% confidence intervals ranged from 1.13 to 3.14. This indicates that the CM+JF combination is consistently more effective across the parameter grid than would be expected from the simple combination of the effects of the individual components.

The most pronounced positive absolute synergy was achieved at high values of *PD* and *WSAR*. At *PD* = 0.90 and *WSAR* = 1.00, the mean value of D_{diff} reached 18.10 (95% confidence interval [17.87; 18.33]), and the corresponding mean synergy index was *S* = 3.27 (lower 95% bound 3.14). In practical terms, this means that while CM and JF acting separately led, on average, to 3.23 and 6.03 destroyed targets, respectively (sum 9.27), their combination resulted in 27.36 destroyed targets per simulation run.

Table 2 summarizes the five parameter combinations with the highest mean value of D_{diff}. In all these cases, the 95% confidence intervals for D_{diff} were unambiguously positive. At the same time, no bootstrap realization with $D_{\text{diff}} \leq 0$ was observed for any of these combinations, corresponding to a one-sided p-value of less than 1.4×10^{-4} (and less than 2.9×10^{-4} for a two-sided assessment). The p-values were derived as the proportion of bootstrap realizations for which $D_{\text{diff}} \leq 0$ held under the one-sided criterion.

Table 2.

Five Highest Mean Values of D_{diff}

PD	0.90	0.90	0.80	0.70	0.90
WSAR	1.00	0.75	1.00	1.00	0.50
N	1500	1500	1500	1500	1500
D_{CM}	3.23	3.16	3.14	2.95	3.13
D_{JF}	6.03	6.01	6.00	5.95	5.97
$D_{\text{CM+JF}}$	27.36	27.10	24.91	23.25	22.76
D_{diff}	18.10	17.94	15.78	14.35	13.66
95% CI for D_{diff}	[17.87; 18.33]	[17.74; 18.14]	[15.58; 15.98]	[14.18; 14.52]	[13.46; 13.87]
S	3.27	3.27	3.04	2.88	2.79
lower 95% CI for *S*	3.14	3.14	2.90	2.75	2.66
p-value (one-sided)	$< 1.4 \times 10^{-4}$	$< 1.4 \times 10^{-4}$	$< 1.4 \times 10^{-4}$	$< 1.4 \times 10^{-4}$	$< 1.4 \times 10^{-4}$
p-value (two-sided)	$< 2.9 \times 10^{-4}$	$< 2.9 \times 10^{-4}$	$< 2.9 \times 10^{-4}$	$< 2.9 \times 10^{-4}$	$< 2.9 \times 10^{-4}$

The box plots for *WSAR* = 1.00 and *PD* = 0.70, 0.80, and 0.90 (Figs. 2a–c) further show that the distribution of the number of destroyed targets in the CM+JF mode is systematically shifted towards higher values compared with the CM and JF modes, while the differences between the modes become clearly more pronounced with increasing *PD*. This is consistent with the intensity map of D_{diff} (Fig. 1) as well as with the values reported in Table 2.

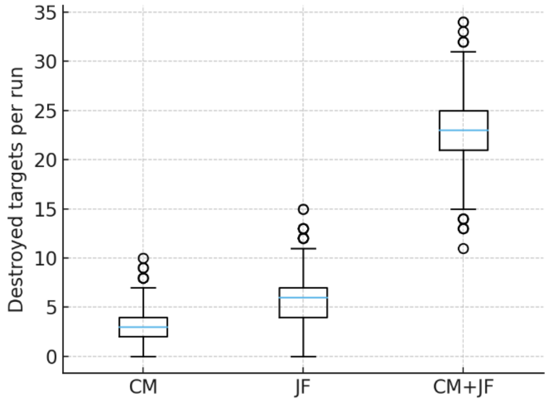

a) *PD* = 0.70; *WSAR* = 1.00

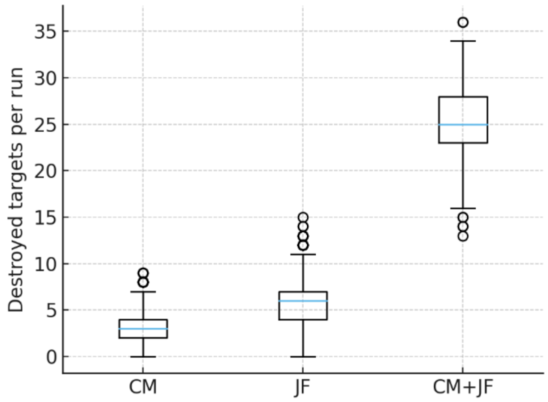

b) *PD* = 0.80; *WSAR* = 1.00

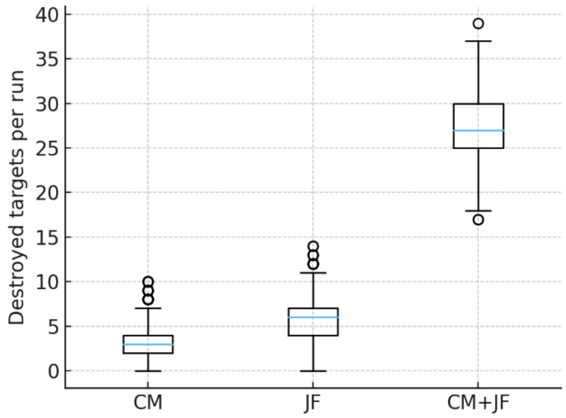

c) *PD* = 0.90; *WSAR* = 1.00

Fig. 2. Distribution of the number of targets destroyed per replication for the three operational modes (CM, JF, CM+JF) at selected values of *PD* and *WSAR*.

The box plots illustrate the distribution of the number of targets destroyed across individual replications for (i) CM alone, (ii) JF alone, and (iii) the combined CM+JF mode. The median is indicated by the horizontal line inside the box, the box represents the interquartile range, and the whiskers denote the range excluding outliers. Outliers are shown separately. The plots document not only the shift in the central tendency under the combined CM+JF mode, but also the variability of the outcome across replications.

5. Discussions

The results show that the combination of counter-mobility measures and fires exhibits a systematically non-additive effect, meaning that the joint effect exceeds the simple sum of the partial effects. Across the entire parameter grid examined, the synergy index *S* has a 95% confidence lower bound greater than 1, indicating that the observed synergy is not a random phenomenon but a stable feature within the selected model. At the same time, it is evident that the magnitude of the synergy is not constant and varies substantially with the parameters *PD* and *WSAR* (Fig. 1).

In terms of the magnitude of absolute synergy, expressed by the difference D_{diff}, the highest values are concentrated in the region of high *PD* and high *WSAR* (Fig. 1 and Table 2). The highest mean value of D_{diff} reaches approximately 18 targets destroyed per run at the combination *PD* = 0.90 and *WSAR* = 1.00. Even in the other best-performing configurations (Table 2), D_{diff} remains at approximately 14–17, indicating that the benefit of the combined action may be substantially greater than that of isolated measures. By contrast, under extremely unfavorable conditions (especially at *PD* = 0), D_{diff} remains around zero and its 95% confidence interval also includes negative values, corresponding to a situation in which the system lacks the conditions necessary for synergy to emerge (typically because the conditions for effective fires are absent).

The synergy mechanism captured by the model corresponds to generally accepted operational logic: counter-mobility measures create time and predictability, while fires convert that time into increased effect. In other words, delay, reduced speed, or channelization of movement increases the engagement window and improves the conditions for target engagement, particularly when detection is sufficient (*PD*) and the availability of assets for engagement is ensured at the same time (*WSAR*). This mechanism is reflected not only in the mean values (Fig. 1), but also in the distribution of outcomes across individual runs (Figs. 2a–c): the CM+JF combination reaches markedly higher values than CM alone and JF alone, and the difference is not driven by isolated extremes but by a shift in the entire distribution.

The relationship between relative and absolute synergy is also noteworthy. The index *S* increases with the parameters *PD* and *WSAR* to values of approximately 3.2–3.3 (Fig. 1), indicating that the combined action may, on average, be several times more effective than would be expected based on a simple sum. At the same time, the absolute difference D_{diff} shows that, under favorable conditions, this relative increase translates into practically significant differences in the number of targets destroyed. For planning purposes, it is important that *S* provides information on nonlinearity, whereas D_{diff} reflects the magnitude of the impact. Together, they therefore make it possible to distinguish situations in which synergy is formally present but operationally insignificant from those in which synergistic action has a decisive effect.

The limitations of the model are primarily related to the simplified description of tactical adaptation and to the abstraction of internal processes. The results should therefore be understood primarily as a quantification of the underlying principle (the non-additive combination of counter-mobility measures and fires) and as a sensitivity map with respect to the parameters *PD* and *WSAR*, rather than as a direct prediction of a specific event. For the purposes of this article, however, this level of abstraction is precisely what makes the model useful. It allows the main message to be situated within the broader context of contemporary defense challenges, while at the same time leaving room for subsequent refinement of the scenario (for example, by explicitly incorporating the stopping rule after a given number of losses, the time components of breach creation, and the differing vulnerability of the target while moving and while halted).

6. Conclusions

This paper addressed the quantification of the non-additive effects of the integrated application of counter-mobility measures and fires in defense. Based on a Monte Carlo simulation conducted in MATLAB 2025a, the individual effects of obstacles, the individual effects of fires, and their combination were compared across a parameter grid defining target detection quality and the availability of fire assets.

The results demonstrated that the CM+JF combination exhibits systematically positive synergy: the synergy index *S* was greater than 1 for all evaluated parameter combinations, confirming that the effect of the integrated action cannot be adequately described as the simple sum of the partial effects. Absolute synergy, expressed by the metric D_{diff}, was positive across most of the parameter space, and its magnitude increased markedly with the simultaneous increase in *PD* and *WSAR*. The highest values of D_{diff} were achieved under conditions of high adversary delay combined with the rapid application of fires. In the most favorable case, the mean value of D_{diff} reached approximately 18 targets destroyed per simulation run.

The study conclusions emphasize that the decisive factor is not merely the effect of obstacles or the effects of fires considered separately, but above all the ability to convert adversary delay into timely and effective fires. In other words, synergy arises when temporal continuity between the obstacle effect and the fire response is ensured; where fire availability is low or the level of detection is insufficient, the system approaches additive behavior, and the synergistic potential remains unexploited.

The paper thus provides a quantitative framework for assessing integrated defense, enabling variants to be compared both in terms of the absolute impact measured by D_{diff} and the relative effect captured by the index *S*. Future work should extend the model in particular by incorporating a more detailed representation of adversary adaptation, explicit temporal dependencies in the fire response, and scenario variants involving additional types of obstacles and different breaching procedures, in order to transfer the insights gained to a broader range of operational conditions.

Practical Implications for National Defense. The results have direct relevance for defense planning based on the integration of counter-mobility measures and fires. The identified non-additive nature of the effect means that the effectiveness of the defense system is determined not only by the quantity of obstacles or the intensity of fires considered separately, but above all by the quality of their temporal and informational linkage. In practical terms, this means that the same physical counter-mobility measure may in one case represent only a temporary delay, while in another it becomes a catalyst for high fire effectiveness, provided that rapid and reliable target identification and engagement are ensured.

It further emerges that the greatest increase in absolute synergy occurs under conditions in which both a high level of adversary delay and a high capability for timely fires are achieved simultaneously. In operational terms, this corresponds to a situation in which the obstacle not only restricts movement but also creates a predictable maneuver and a sufficiently long-time window for engagement. By contrast, under conditions of low fire availability or a low level of detection, the synergistic potential decreases and the integrated system approaches additive behavior. This underscores the importance of coordination and synchronization among force elements, particularly with respect to the temporal dimension of the action.

The results also support a practical distinction between the relative and absolute expression of synergy. The synergy index *S* provides information on the degree of non-additivity and appropriately captures the trend of increasing effect with rising *PD* and *WSAR* values, whereas D_{diff} expresses the magnitude of the added effect and thus the practical significance of coordinated action. The combination of both metrics makes it possible to assess integrated defense variants not only in terms of whether synergy is present, but also in terms of whether it has a meaningful effect under the given operational conditions.

Acknowledgements. The authors thank the organizers of CNDCGS 2026 for providing the opportunity to present this research. This work was conducted within the framework of the projects "Battle field 2030+" and "Conduct of land operations (LANDOPS)".

References

1. **Gilli A., Gilli M., Grgić G.** NATO, Multi-domain operations and the future of the Atlantic Alliance. Comparative Strategy, 2025, 44:1, p.73–91.
2. Strategic Foresight Analysis 2023. Allied Command Transformation. Norfolk. 2023.
3. **Palasiewicz T., Rolenec O., Lacinová V., Bilina M.** A Simulation-based analysis for optimal placement of anti-tank obstacles in armored warfare. Journal of Defense modeling and Simulation, 2025, 15485129251339485.
4. (ATP-3.12.1) Tactical Doctrine for Engineering. NATO Standardization Office. Brussels. 2023.
5. (JP 3-15) Barriers, Obstacles, and Mine Warfare for Joint Operations. Department of the Army. Washington DC. 2018.
6. **Hrnčiar M., Kompan J., Nohel J.** The future of the battlefield: Technology-driven predictions in the land domain. Revista Científica General José María Córdova, 2025, 23(49), p.277–296.
7. (JP 3-09) Joint Fire Support. Department of the Army. Washington DC. 2010.
8. **Green K.L.** Complex Adaptive Systems in Military Analysis. Institute for Defense Analyses, 2011.
9. (AJP-3.2) Allied Joint Doctrine for Land Operations. NATO Standardization Office. Brussels. 2022.
10. (AJP-3.9) Allied Joint Doctrine for Joint Targeting. NATO Standardization Office. Brussels. 2021.
11. **Šustr M., Ivan J., Blaha M., Potužák L.** A Manual Method of Artillery Fires Correction Calculation. Military Operations Research, 2022, 27(3), p.77–94.
12. **Drábek J., Šustr M., Potužák L., Ivan J., Liška R.** Contingency and Emergency Manual Procedures for Calculation Firing Data Using Direction and Distance Coefficients. Engineering Reports, 2025, 7(6), e70252.
13. **Washburn A., Kress M.** Combat Modeling. Springer, 2009.
14. **Przemieniecki J.S.** Mathematical Methods in Defense Analyses. American Institute of Aeronautics and Astronautics, 2000.
15. **Palasiewicz T., Skalický P.** The Possibilities of Antitank Mine-Laying with Mine Delivered Systems. Vojenské rozhledy, 2017, 26 (1), p.109–117.
16. **Palasiewicz T., Kyjovský J.** Criteria Determination for Obstacle Effectiveness Evaluation. Proceedings of The 23rd International Conference The Knowledge-Based Organization. Sibiu, 2017, p.227–232.
17. Summary of the Joint All-Domain Command and Control (JADC2) Strategy. Department of Defense, 2022.
18. **Lingel S., Sargent M., Gulden T.R., McDonald T., Rockstroh P.** Leveraging Complexity in Great-Power Competition and Warfare: Volume II, Technical Details for a Complex Adaptive Systems Lens. RAND Corporation, 2021.
19. **Middleton V.** Simulating Small Unit Military Operations with Agent-Based Models of Complex Adaptive Systems. Proceedings of the 2010 Winter Simulation Conference. Baltimore, 2010, p.119–134.
20. **Cioppa T.M., Lucas T.W., Sanchez S.M.** Military Applications of Agent-Based Simulations. Proceedings of the 2004 Winter Simulation Conference. Washington DC, 2004, 171–180.
21. **Brown L.P., Cioppa T.M., Lucas T.W.** Agent-Based Simulations Supporting Military Analysis. Phalanx, 2004, 37(3), p.29–32.
22. **Rubinstein R.Y., Kroese D.P.** Simulation and the Monte Carlo Method: Third Edition. John Wiley & Sons, 2011.